Using a Building as Thermal Storage and Model Predictive Control of a Heat Pump for Grid Stabilization

Master's thesis of

Vivien Geenen

at the Department of Mechanical Engineering
Institute for Automation and Applied Informatics (IAI)

Reviewer:	Prof. Dr. Veit Hagenmeyer
Second reviewer:	apl. Prof. Dr. Jörg Matthes
Advisor:	Moritz Frahm, M.Sc. and Frederik Zahn, M.Sc

14. June – 14. December 2021

I declare that I have developed and written the enclosed thesis completely by myself, and have not used sources or means without declaration in the text.

PLACE, DATE

. . . . . .

(Vivien Geenen)

Kurzfassung

Abstract

Contents

List of Figures

List of Tables

1. Introduction

Climate change is challenging the entire world. In the Paris Agreement, the United Nations (UN) agrees to keep the rise in global average temperature significant under two degrees Celsius [1]. To achieve this aim every nation has to reduce its greenhouse gas emissions. This calls for changes in the mobility sector, industry, and energy production, for example. Germany intends to implement this by promoting electromobility, using hydrogen in industry, and energy transition [2]. In particular, the energy transition that has already been initiated has to be driven forward. That means the expansion of renewable energies and decreasing conventional power plants. The German government is aiming to phase out coal-fired power plants by 2038 [3]. For covering the energy demand, a high increase in photovoltaics and wind power is necessary in a few years.
Unfortunately, a disadvantage of this renewable energy is that they fluctuate with the weather and do not release energy by demand. In addition, more renewable energies lead to more intense instabilities in the grid. In the first solution approach, energy storage and demand side management (DSM) are used to implement the stable grid in the future. Batteries, pumped hydroelectric energy storage, thermal energy storage, and much more could store an excess of power during a sunny or windy day. Further, DSM is clever adding and removing loads from the grid per demand and results in smoothing the grid. Load shifting is part of DSM [4] and already used industrial. A new approach is to use residential buildings as thermal storage and demand response to contribute to grid stability. Particularly the idea of controlling the heat pumps of buildings seems promising. As at least 1.25 million heat pumps are already installed in Germany, and the tendency is increasing [5].
The implementation of this approach needs a control strategy ensuring consumer comfort. Using the weather forecasts and prediction of the grid fluctuations improve the control. Model predictive control (MPC) is one suitable instrument to integrate forecasts and control heat pumps in buildings for stabilizing the grid with the thermal storage of the building. Research has already shown the possibilities of MPC to shift loads, to save energy and costs. This

thesis goes in detail with the differences in consumption, comfort and grid-services with and without an occupancy plan of the building.

1.1. Objective of this work

This thesis aims to design a control system, which simultaneously serves the grid and comply with the required comfortable internal temperature range, for the heat pump of a building in the so-called "Living Lab" of the Karlsruhe Institute of Technology (KIT) at Campus North. The implementation is to be carried out using the control method Model Predictive Control. This method enables to predict the future thermal behaviour of the building and to react to the actual and future fluctuations of the weather or the grid for example. In the first step, a thermal model of the building behaviour must be created. For this purpose, the RC analogy is to be used. To reduce the complexity of the thermal behaviour of the building, appropriate assumptions can be made. Furthermore, the resulting model should correspond to a grey-box model, i.e., a middle ground between exact and black-box model description. After the verification of the thermal model using measured data from the Living Lab, an optimal control problem shall be created. The aim is to construct an MPC algorithm and to simulate its application. The software used will be Matlab/Simulink.

1.2. Related work

Extant literature investigates thermal modelling and controlling of buildings. Kramer et al. [6] summarize in a literature review thermal modelling approaches such as white-box, grey-box, and black-box models and present how researchers apply these approaches. Authors identify their thermal model parameters with measurements [7],[8], [9], like a grey-box model or use grey-box models [10], [11]. Coakley et al. [12] see the advantages in the short development time for the model, fidelity of predictions, and the interaction of building, system and environmental parameters. One disadvantage is that modellers need a high level of knowledge in physical and statistical modelling [12].
Further, some authors work with such thermal models in their MPC applications for thermal management in buildings [13], [14].
Regardless of the type of model, MPC is utilised for control of heating, ventilation, and air conditioning (HVAC) systems in buildings for a variety of reasons. Researchers are interested

in the reduction of energy consumption [14] and saving costs [15] while obtaining thermal comfort. Some studies present how to decrease or shift the peak load of buildings [16].
On the other hand, some articles refer to the potential of heat pumps for grid services. The report "Wärmepumpen in Bestandsgebäuden" examines, among other things, the load shifting potential of grouped heat pumps. The researchers determine 4 to 14 GWh load shifting potential for one million heat pumps [17]. Kohlhepp and Hagenmeyer [18] also analyse the flexibility of heating systems for smart grids, partially of heat pumps.
The researchers apply the above topics grey-box modelling and MPC for heat pumps to the realization of grid-services. Thus, they address thematically DSM. The paper by Avci et al. [19] gives an early indication of the potential of grid-services using real-time pricing. In the meantime, many research papers deal with prices whereby the focus in the papers differs e.g. according to the type of buildings [20], [21] or the type of optimisation [20], [22].
Another interesting part of research is the energy saving potential by planing the occupancy of buildings. Wang et al. show in their paper that 13 percent of energy can be saved by occupancy-based controls for an office building [23]. Researchers are trying to find out how to predict an occupancy schedule with for example machine learning approaches to better control of HVAC and consequently to save energy [24].

However, is their effort necessary for an MPC with the aim of grid-services? A simple occupancy plan should be used to examine whether comfort, grid services and energy consumption can be improved compared to an MPC without an occupancy plan. Consequently, in this thesis, an MPC is created with a grey-box model and grid services are implemented with real-time pricing, similar to the papers above. However, the potential of an occupants schedule is analysed at a real reference building during focusing on the aim of grid services. This thesis finds an answer to the question: How is the difference between a view with occupants schedule and without concerning grid-services, energy consumption and comfort?

1.3. Content structuring

Stukturierung meiner Thesis erläutern

2. Foundations

This work is based on foundations, which are summarized in this chapter. This includes thermal basics, foundations about thermal modelling, and model predictive control (MPC).

2.1. Thermal basics

2.1.1. Balancing energy

It is necessary to comprehend the basics of thermodynamics to understand the structure of a thermal model. The first law of thermodynamics is the general energy balance and is formulated for unsteady and open systems as follows [25]:

$$\sum_i \dot{Q}_\mathrm{i} + \sum_j \dot{W}_\mathrm{j} + \sum_k \dot{m}_\mathrm{k} * (h + \frac{c^2}{2} + gz)_\mathrm{k} = \frac{d}{dt} \sum_l U_\mathrm{l} \tag{2.1}$$

In terms of a building, we set the work $\dot{W}$ to zero according to the relationship $W = \int Pdt - \int pdV$ [25] because a building can't change the volume V, and we have no additional mechanical power P. If we have no mass flow $\dot{m}$ in our system, we obtain a closed system. Regarding buildings, mass flows could be airflow through the window, for example. Then we also consider the enthalpy h, the fluid velocity c, the high z and the gravitational acceleration g.
Since we do not consider airflow, we use the closed system with the heat flows $\dot{Q}_\mathrm{i}$ and the inner energy U_l.

$$\sum_i \dot{Q}_\mathrm{i} = \frac{d}{dt} \sum_l U_\mathrm{l} \tag{2.2}$$

The deduction of the inner energy U starts with the complete differential description of the specific inner energy du as [25]:

$$du = (\frac{\partial u}{\partial T})_{\mathrm{v}} dT + (\frac{\partial u}{\partial v})_{\mathrm{T}} dv \tag{2.3}$$

The specific volume dv is negligible in buildings, and the specific heat capacity during constant volume has the expression $c_{\mathrm{v}} = (\frac{\partial u}{\partial T})_{\mathrm{v}}$ [25]. After integrating and replacing the specific values by volume, we obtain the relation for the inner energy U, with the mass m and the temperature difference δT.

$$U = m c_{\mathrm{v}} \Delta T \tag{2.4}$$

It applies to substances with a specific volume regardless of the pressure that $c_{\mathrm{v}} = c_{\mathrm{p}} = c$. We sum the heat flows in the energy balance in Equation 2.2. However, what kind of heat transfer is there, the following few chapters explain.

There are three mechanisms of heat transfer: Heat conduction, heat convection, and heat radiation [26]. Thermal modelling of buildings requires all of these mechanisms. For example, conduction is the primary part of heat transfer through walls or floors. Convection occurs on the inside and the outside of the building between the walls and the air. To integrated the impact of the sun, radiation is needed, for example.

2.1.2. Conduction

Conduction means that heat energy is directed in a solid or fluid. Molecules within the solid or fluid have higher energy when the temperature is higher. They transfer the energy to neighbouring molecules with smaller energy. Without a heat source, the temperature difference between a hot and a cold location of the molecules decreases.[27]
The equation

$$\dot{\mathbf{q}} = -\lambda \nabla T \tag{2.5}$$

describes the conduction according to Fourier [26]. There is λ the thermal conductivity with the assumption of being constant and $\dot{\mathbf{q}}$ and T represent the specific heat flux and the temperature. The thermal conductivity is dependent on the material, such as concrete, wood

or bricks.
To know the heat flux $\dot{Q}$, it is necessary to expand the above equation with the area A, the thickness of the conductive medium d and a temperature difference ΔT assuming one significant direction of the heat flux $\dot{Q}$ to:

$$\dot{Q} = \frac{A\lambda}{d}\Delta T \tag{2.6}$$

In terms of buildings, the conductive medium could be walls, floors or roofs.

2.1.3. Convection

Macroscopic movements of a fluid lead to the transport of kinetic energy and enthalpy. This mechanism is called convection. These movements are generated by external forces or by internal forces like balancing the pressure or temperature.[26]
Newton's law of cooling describes the convective heat transfer $\dot{Q}$ as

$$\dot{Q} = \alpha A(T_w - T_\infty) \tag{2.7}$$

with the heat transfer coefficient α , especially for building modelling the wall temperature T_w and the environment temperature T_∞ [28] . There are two possibilities to determine the heat transfer coefficient. Both require a temperature difference ΔT and either a temperature gradient $\partial T/\partial x$ or a heat flux $\dot{Q}$. [26]

2.1.4. Radiation

Every body emits heat radiation to the environment with electromagnetic waves. Especially, heat radiation does not need matter for energy transportation. As shown in the following equation, the temperature T of the body influences heat radiation.[26]

$$\dot{q} = \sigma T^4 \tag{2.8}$$

This correlation applies to a black body, where $\dot{q}$ is a heat flux and σ represents the Stefan-Boltzmann coefficient. A black body absorbs all heat radiation with all wavelengths from all directions[28]. The consideration of a black body is idealized. For the illustration of a real

body (see Equation 2.9), the emissivity ϵ is used. ϵ is material-dependent and lies between 0 and 1.

$$\dot{q} = \epsilon \sigma T^4 \tag{2.9}$$

In general, a body absorbs, transmits, and reflects radiation with the appropriate coefficients a, τ and r. The sum of three coefficients has to be one ($a + \tau + r = 1$) [29].
The primary source of heat radiation is the sun, which plays an important role in the thermal modelling of buildings. Objectives in the building, such as radiators, also radiate heat. For example, radiators have equal parts convective and radiative energy transport [8].

2.2. Lumped capacitance model

For modelling the thermal behaviour of buildings, the lumped capacitance model is often used. With this approach, using the electrical analogy, building elements are represented by resistors R and capacitors C. [6]

2.2.1. Electrical analogy

Similar to an electrical network, the potential is represented by the temperature at one node and the heat flux corresponds to the current. We can also use Ohm's law, which is formulated in a thermal way as:

$$\dot{Q} = \frac{\Delta T}{R} \tag{2.10}$$

Combining the above equation with Equation 2.6 or Equation 2.7, the thermal resistance R is determined in conductive cases as [27]:

$$R_\lambda = \frac{d}{A\lambda} \tag{2.11}$$

and in convective cases as[28]:

$$R_\alpha = \frac{1}{\alpha A} \tag{2.12}$$

Thermal resistances can sum up to one thermal resistance, even if they are from different mechanisms of heat transfer. Based on an example in Figure 2.1, the addition is explained. The figure shows a section of a wall with a heat flow $\dot{Q}$, the ambient temperature T_1 and T_2 separated by that wall. We have three thermal resistances $R_{\alpha,1}$, $R_{\alpha,2}$, and R_λ, which we sum to one thermal resistance $R = R_{\alpha,1} + R_\lambda + R_{\alpha,2}$. Now, we can calculate the heat flow $\dot{Q} = \frac{T_2 - T_1}{R}$ according to Equation 2.10.

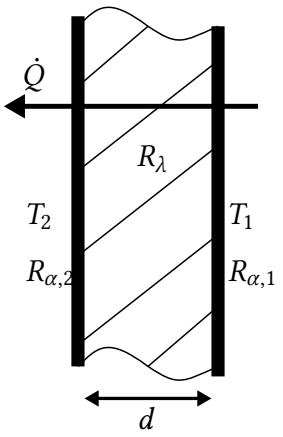

Figure 2.1. Sample of a wall with thermal resistances

In sum, the thermal resistances R comply with electrical resistors. Further for modelling thermal networks, the thermal capacitance C is needed. It is calculated from the specific heat capacity c multiplied by the mass m ($C = cm$).
For a better explanation of the structure of a thermal network, a simple example is depicted in Figure 2.2. It represents a heated wall of a building. The heat flux $\dot{Q}$, for example from a

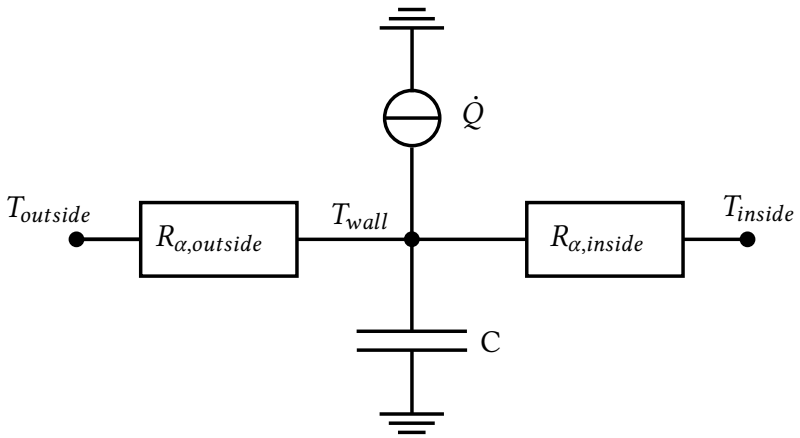

Figure 2.2. Sample RC- network

radiator, influences the temperature T_{wall}, as well as the capacitance C. And the temperature T_{wall} affects the temperature inside and outside T_{inside} and T_{outside} with their resistances $R_{\alpha,\text{inside}}$ and $R_{\alpha,\text{outside}}$. The example shows that all connections in the network influence each other. To model the dynamics of the wall in differential equations, Kirchhoff's Current Law is required.

It states that the sum of the flowing current to the node is equal to the sum of the flowing current of the node [27]. Because of the thermal analogy of electrical laws, the current is replaced by heat flux. The following differential equation results for the node T_{wall} using Ohm's law ($\dot{Q} = \Delta T/R$) and the relationship $\dot{Q} = C\frac{\partial T}{\partial t}$.

$$C\frac{\partial T_{\text{wall}}}{\partial t} = \dot{Q} + \frac{T_{\text{inside}} - T_{\text{wall}}}{R_{\alpha,\text{inside}}} - \frac{T_{\text{wall}} - T_{\text{outside}}}{R_{\alpha,\text{outside}}} \tag{2.13}$$

In Figure 2.2, the thermal resistances are serially connected. According to the electrical network, resistances in series are equal to their sum.

$$R_{\text{sum}} = R_{\alpha,\text{inside}} + R_{\alpha,\text{outside}} \tag{2.14}$$

A parallel circuitry has windows and walls in buildings, for example. Here the resistances are calculated according to the following schema:

$$\frac{1}{R_{\text{sum}}} = \frac{1}{R_{\text{wall}}} + \frac{1}{R_{\text{window}}} \tag{2.15}$$

In terms of needed more capacitances for describing the thermal model, the summary capacitance is added in a parallel circuitry as:

$$C_{\text{sum}} = \sum_{1}^{i} C_{\text{i}} \tag{2.16}$$

The serial circuitry of capacitances is calculated as follows:

$$\frac{1}{C_{\text{sum}}} = \sum_{1}^{i} \frac{1}{C_i} \tag{2.17}$$

2.3. Model predictive control (MPC)

Model predictive control exploits models of the plant to predict and optimise the behaviour of the plant [30]. Applied to thermal control of a building with the aim of grid-supporting, a model of the thermal behaviour of the building is required to predict the reaction of the system behaviour in the next N time steps, called the prediction horizon. Every time step k, the current state $\mathbf{x_k}$, the output $\mathbf{y_k}$ is measured, and the future system behaviour is obtained

by computation. The computation of the future system behaviour may include measurable disturbances such as weather forecast, occupancy schedule and the optimisation of the control signal $\mathbf{u_k}$ over the optimisation horizon $\mathbf{u_{k+N}}$. However, only the first calculated control signal is adopted as input for the plant. Then, the calculations are repeated at every time step. Figure 2.3 visualises the MPC control loop.

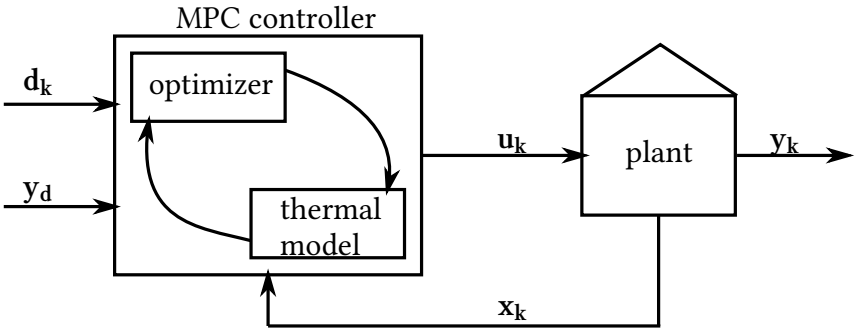

Figure 2.3. MPC structure of the control loop

Concluded, the MPC is "an iterative online optimisation over the predictions" [30] compiled by the thermal model of the building. Mathematically explained, the optimizer needs to minimize the following equation according to [31] and [32]:

$$\text{Cost function} \qquad \text{minimize} \sum_{k=1}^{N-1} c_k(\mathbf{x_k}, \mathbf{u_k}, \mathbf{y_k}) \tag{2.18}$$

subject to

$$\begin{aligned}
\text{Current state} \quad & \mathbf{x_0} = \mathbf{x} \\
\text{Dynamics} \quad & \mathbf{x_{k+1}} = f(\mathbf{x_k}, \mathbf{u_k}, \mathbf{d_k}) \qquad \mathbf{y_k} = g(\mathbf{x_k}, \mathbf{u_k}, \mathbf{d_k}) \\
\text{Constraints} \quad & \mathbf{y_{min}} \leq \mathbf{y_k} \leq \mathbf{y_{max}} \\
& \mathbf{u_{min}} \leq \mathbf{u_k} \leq \mathbf{u_{max}}
\end{aligned}$$

c_k represents the cost function, which is explained in detail in subsection 2.3.1 . In terms of building control, y is the internal temperature.

	m	n
A	number of states	number of states
B_1	number of states	number of control signals
B_2	number of states	number of disturbances
C	number of outputs	number of states
D_1	number of outputs	number of control signals
D_2	number of outputs	number of disturbances

Table 2.1. dimensions of the matrices

2.3.1. Cost function

Generally, the cost function c_k assigns a cost to the control signal $\mathbf{u_k}$ and the current state $\mathbf{x_k}$, which is mathematically described in Equation 2.18 , with:

$$c_k = (\mathbf{x_k^T} Q \mathbf{x_k} + \mathbf{u_k^T} R \mathbf{u_k}) \tag{2.19}$$

Here Q and R are matrices over which individual elements of the state vector or control signal vector can be weighted differently. [33] Especially for every application, the cost function has an individual form to reach the aims of the MPC.

2.3.2. Dynamics

The state-space formulation (SSF) is an alternative representation of a linear differential equation, which models a physical system. In this work, it is used for the formulation of the thermal model, which is required for the MPC. The SSF consists of the state $\mathbf{x}$, the control signal $\mathbf{u}$, the disturbances $\mathbf{d}$ and the output of the system $\mathbf{y}$ are represented in Equation 2.20. The system matrix is A, B_1 and B_2 are called the input matrices, C is the output matrix, D_1 and D_2 are the pass-through matrices. The Table 2.1 lists the dimensions of the matrices m x n with m rows and n columns.

$$\begin{aligned} \dot{\mathbf{x}} &= A\mathbf{x} + B_1\mathbf{u} + B_2\mathbf{d} \\ \mathbf{y} &= C\mathbf{x} + D_1\mathbf{u} + D_2\mathbf{d} \end{aligned} \tag{2.20}$$

Every differential equation needs initial values for solving. Therefore, initial states $\mathbf{x_0}$, initial control signals $\mathbf{u_0}$, and initial disturbances $\mathbf{d_0}$ must be given. In a thermal model of a building, some authors ([8], [7]) use the state as a vector of some temperatures, the control

signal as a signal for the heating system, the disturbances can describe the influence by the weather or occupants and the output of the system contains frequently the temperature inside of the building.

2.3.3. Constraints

Dealing with constraints is one of the most important advantages of MPC. Thereby, constraints can be used for the state, the output, and the input. In terms of building control, output constraints and input constraints are reasonable, as mathematically described in the Equation 2.18. That means, the output constraints could be a temperature range, which feels comfortable for occupants. And the constraints for the input are given as minimal (= 0) and maximal values of the possible performances. General, logical and physical ranges are constrained. There are different forms of constraints, but linear constraints are frequently used for MPC because they simplify the optimisation problem. Constraints can also be time dependant. This is beneficial for embedding diverse temperature ranges during the night and the day or during the working time of occupants when they are not at home. [7]

2.4. The reference building

Since this thesis is based on a real building, some necessary details about the building are described below.
The building is located on the "Campus Nord" of the Karlsruhe Institute of Technology and is part of the "Energy Lab 2.0", "a research infrastructure for renewable energy"[34]. It is equipped with a kitchen, a bathroom, five rooms and a technical room. For a better orientation, Figure 2.4 shows a part of the construction plan of the building. The building is designed as a single-family house, but for practical reasons, it is used as an office. The living area is around 100 m^2. The building offers two options to heat or cool with a ground-source heat pump or an air heat pump. The focus is on the air heat pump because the most commonly used heat pumps in Germany are air heat pumps [35]. In addition to the heat pump, there is a water reservoir for saving energy with stratified storage. The total volume is 1000 litres [36]. The heating system inside the building is provided as underground floor heating. However, the heating system is not completely installed yet. So using the heat pump, the water reservoir or the underground floor heating is not possible actual.
One of the main features of the building is the number of sensors. The air temperature

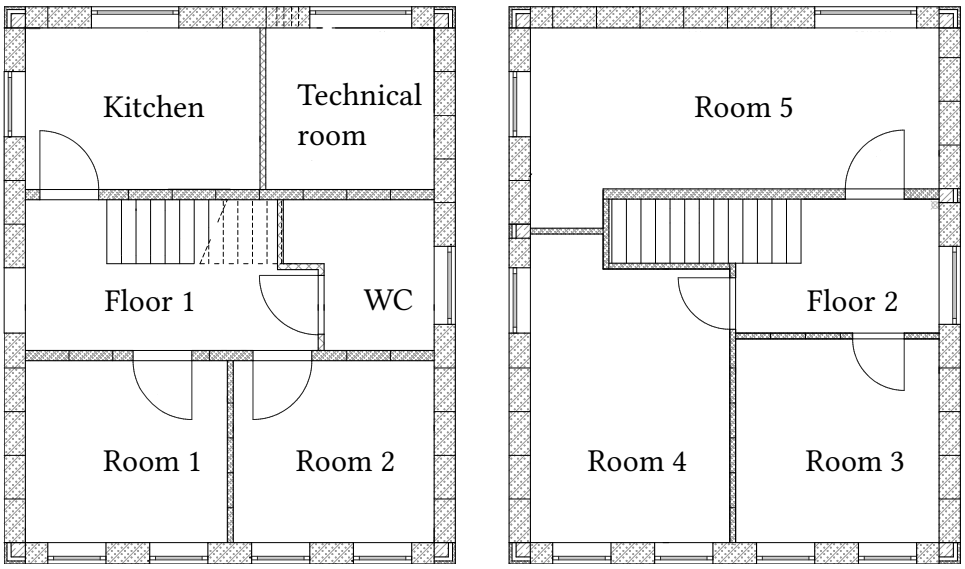

Figure 2.4. Construction plan of the building [37]

is measured in every room, as well as the temperature in the middle of the exterior wall, the screed temperature, the floor plate temperature, and the temperature of the inner wall between room three and room four (see Figure 2.4). Furthermore, the consumption of the actual electrical power is also detected. Only the mentioned sensors are needed in this case, but there are many more sensors.

3. Modelling

After explaining thermal basics and the electrical analogy, the foundations are used in this chapter. The creation of the thermal model of the reference building and the resulting thermal model are presented. Later, the model is needed for the MPC to predict the thermal reactions of the building.

The focus of this work is on the MPC part, so a simple thermal model is required. Nevertheless, no necessary information must be missing. Therefore, the thermal storage possibilities, the temperature inside of the building, and the heating system's influence have to be represented in the model. The storage allows to heat during the grid has too much power and to save energy in the building during the grid requires power. Hence, this enables the MPC's objective of grid services. The output of the model needs to be the temperature inside since the MPC aims to be in a pleasant temperature range to ensure customer comfort. Last, the influence of the heating system must be recognisable in the model, as it is the input of the plant.
The thermal model records the thermal conditions of the reference building. Therefore, the inner energy of the water reservoir and the air temperature inside the building are modelled. The water reservoir and the building behaviour are modelled according to different modelling strategies. The following chapters describe the partial models water reservoir and building model, the kind of modelling, and the conclusion of the partial models.

3.1. The modelling strategies

Creating a model can be made with three types of models, the so-called white-box models, grey-box models or black-box models. White-box models describe the real system only physically. Black-box models, on the other hand, have no physical description. They are created with data. And grey-box models are in between these two options [38]. All possibilities are used in the thermal modelling of buildings [6].

The chosen approach for the MPC is the **grey-box model** for two reasons: First, this approach combines the advantages of white-box models and black-box models [39]. Second, there is the possibility to generate the required data from the reference building with the available measurement equipment at KIT. According to Coakley et al., further advantages and disadvantages are among other things[12]:

Advantages	Disadvantages
• faster development by a combination of physical and statistical model	• requires knowledge in physical and statistical modelling
• accuracy of the results for the specific use case, provided by qualitative training data	• changes at the building lead to a retraining

Table 3.1. Advantages and disadvantages of grey-box modelling

However, the water reservoir and the heating system are not in use yet. So, no data are available for training a grey-box model. That's the reason why a part of the model needs to create as **white-box model**.
But also, white-box models have some pros and cons (see the following Table [39]).

Advantages	Disadvantages
• relies on physics	• needs assumptions to simplify
• applicable for every situation with the same assumptions and requirements	• often complex mathematical problems

Table 3.2. Advantages and disadvantages of white-box modelling

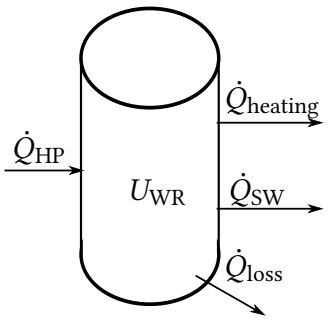

Figure 3.1. Figure of the water reservoir with the heat flows

3.2. The water reservoir model

First, all heat flows are regarded for modelling the water reservoir (WR) , which influence the water reservoir (see Figure 3.1). The heat pump (HP) feeds the water reservoir with heat flow $\dot{Q}_{\text{HP}}$. The service water (SW) and the water for the heating circuit are taken from the storage. Since no service water is currently connected to the reference building, the heat flow $\dot{Q}_{\text{SW}}$ will be set to zero in the following. The heat losses $\dot{Q}_{\text{loss}}$ and the heating heat flow $\dot{Q}_{\text{heating}}$ are consequently the discharged heat flows. The resulting energy balance according to Equation 2.2 follows below.

$$\frac{dU_{\text{WR}}}{dt} = -\dot{Q}_{\text{heating}} + \dot{Q}_{\text{HP}} - \dot{Q}_{\text{loss}} \tag{3.1}$$

Since the model are referred to a real building, the size of the heat flows and the inner energy are limited according to the devices of the building. The heating heat flow moves in a range according to the calculations of the heating system [40] and can also have negative values when cooling is required (then according to the calculations of the cooling load [41]). The heat losses and the heat pump heat range are taken from the technical data [36], [42]. Since the reference water reservoir is a stratified storage we determine the maximum inner energy in assumption of two heat layers. According to Equation 2.4, we need material parameters of water ($c_{\text{v,w}}$, ρ_{w}), the size of the water reservoir ($m = \rho_{\text{w}} V$), both is known, and a temperature difference, which we define for both layers. We assume that we heat up the storage from ambient temperature T_{amb} around 20°C in both layers. Even with negative outside temperatures, the characteristic diagram of the heat pump provides the maximum inlet temperature of 55 °C, which should be the maximum temperature of the upper layer in the water reservoir $T_{\text{max,1}}$. The maximum temperature of the lower layer $T_{\text{max,2}}$ orients

towards the inlet temperature of the underfloor heating and lies by 35 °C. After that, we calculate the sum of the inner energy as follows.

$$U = \rho_{\mathrm{w}} c_{\mathrm{v,w}} ((T_{\mathrm{max},1} - T_{\mathrm{amb}}) * \frac{V}{2} + (T_{\mathrm{max},2} - T_{\mathrm{amb}}) * \frac{V}{2}) \tag{3.2}$$

3.3. The building model

First, a physical description of the thermal dynamics of the building must be created. To obtain the condition of a simple model, we model the building as a single zone, as often practised in the literature [9], [8]. Single zone means that we sum all relevant values of the rooms, such as air temperature or wall temperature, by averaging to one value.
We consider the air temperature, the temperature of the outer walls, the temperature of the inner walls and floors in the first floor, and the temperature of the floor in the model. In the following, these temperatures are called: inside temperature T_{inside}, envelope temperature T_{envelope}, interior temperature T_{interior}, and floor temperature T_{floor}. Using the state-space formulation (see subsection 2.3.2), the temperatures are states in this model. According to the RC-analogy (see subsection 2.2.1), the model is built and nearly explained in the following for every state.

Inside temperature:
One focus lies on the accuracy of the inside temperature since this temperature will be controlled in the later prepared MPC. Therefore, a more precise description of the dynamics is required (see the following equation). We consider the influence of the sun $\dot{Q}_{\mathrm{sun,inside}}$, the heating system $\dot{Q}_{\mathrm{heating}}$ and the other states in the way shown in the following equation. $\dot{Q}_{\mathrm{heating}}$ links the water reservoir model and the building model because the heat flow is the same but leaves the water reservoir model and enters the building model.

$$\begin{aligned} C_{\mathrm{inside}} * \frac{dT_{\mathrm{inside}}}{dt} = \quad & \dot{Q}_{\mathrm{heating}} + \dot{Q}_{\mathrm{sun,inside}} - \frac{T_{\mathrm{inside}} - T_{\mathrm{envelope}}}{R_{\mathrm{inside}}} - \frac{T_{\mathrm{inside}} - T_{\mathrm{outside}}}{R_{\mathrm{window}}} \\ & - \frac{T_{\mathrm{inside}} - T_{\mathrm{interior}}}{R_{\mathrm{interior}}} - \frac{T_{\mathrm{inside}} - T_{\mathrm{floor}}}{R_{\mathrm{floor}}} \end{aligned} \tag{3.3}$$

The detailed explanation for the composition of the thermal resistance and capacitance is in subsection 2.2.1. In the following table, the special material and state dependant values are explained.

C_{inside}	The thermal capacitance C_{inside} is calculated with the mass of the air from all rooms and the capacity of the air (1006 $J/(kgK)$ [43]). The mass can be determined with the volume of the rooms according to the construction plan [37] and the air density (1.28 kg/m^3 [43]).
R_{inside}	The thermal resistances R_{inside} includes a convective part with the transfer coefficient $\alpha = 0.9W/(m^2K)$ special for air perpendicular to the wall in buildings with the assumption of one Kelvin temperature difference between the wall and air [44].
R_{window}	The window resistance R_{window} is determined with the window area and the assumption of a heat transmission coefficient $u = 1W/(m^2K)$ [45].
R_{floor}	Heat conductivity and heat convection are the regarded mechanisms to determine the floor resistance R_{floor}. The floor material is reinforced concrete with the thermal conductivity of $2.3W/(mK)$ [46].
R_{inside}	For the convection in the inner of the building, the same assumptions are made as for R_{inside}.
R_{interior}	The interior resistance R_{interior} is also calculated with the heat transfer coefficient inside.

Table 3.3. Explanation of the special material and state dependant values of the differential equation of the inside temperature

Envelope Temperature:

The sun, the contact of the walls with the inner air temperature and with the outside temperature influence the envelope temperature. The sun affects the air temperature in another area ratio than the outer walls. Therefore, we difference the influence of the sun on the inner air temperature and the envelope, and we consider here $\dot{Q}_{\text{sun,envelope}}$.

$$C_{\text{envelope}} * \frac{dT_{\text{envelope}}}{dt} = \dot{Q}_{\text{sun,envelope}} - \frac{T_{\text{envelope}} - T_{\text{outside}}}{R_{\text{envelope}}} + \frac{T_{\text{inside}} - T_{\text{envelope}}}{R_{\text{inside}}} \tag{3.4}$$

R_{envelope} The outer wall resistance R_{envelope} contains a heat conductivity of aerated concrete ($0,133 W/(mK)$ [47]) and the heat transfer coefficient for air perpendicular to the wall outside α_{envelope} according to the rules of thumb from Schweizer-fn [44]

$$\alpha_{\text{envelope}} = 3,96(v/L)^{0},5 = 1,669 W/(m^2K) \tag{3.5}$$

with the average wind velocity of Karlsruhe v [48] and the length of the building wall.

C_{envelope} To determine the capacitance C_{envelope}, we need the volume of the outer walls from the construction plan [37], the density of aerated concrete ($485 kg/m^3$) and the capacity ($1000\ J/(kgK)$) [47].

Table 3.4. Explanation of the special material and state dependant values of the differential equation of the envelope temperature

Interior and floor temperature:

The differential equations for the interior and the floor temperature are as simple as possible. Both states have just an impact on the inside temperature. Hazyuk et al. models for example also the ground floor as one state [8]. The explanation is that the ground floor has no convective contact with the environment. Therefore, he is not modelled with the envelope for holding the physical structure, where the wind has an impact on the outer walls. The interior is extra modelled to improve the accuracy of the inside temperature equations because the capacitance of the inner walls is specially collected.

$$C_{\text{interior}} \frac{dT_{\text{interior}}}{dt} = \frac{T_{\text{inside}} - T_{\text{interior}}}{R_{\text{interior}}} \tag{3.6}$$

$$C_{\text{floor}} \frac{dT_{\text{floor}}}{dt} = \frac{T_{\text{inside}} - T_{\text{floor}}}{R_{\text{floor}}} \tag{3.7}$$

As above, we need some material parameters for the calculation of the capacitance C_{floor} and C_{interior}. The material of the floor is reinforced concrete and the interior' material is aerated concrete. The previously unnamed material parameters are the density ($2500 kg/m^3$) [46] and the capacity ($880 J/(kgK)$) [49] of reinforced concrete.

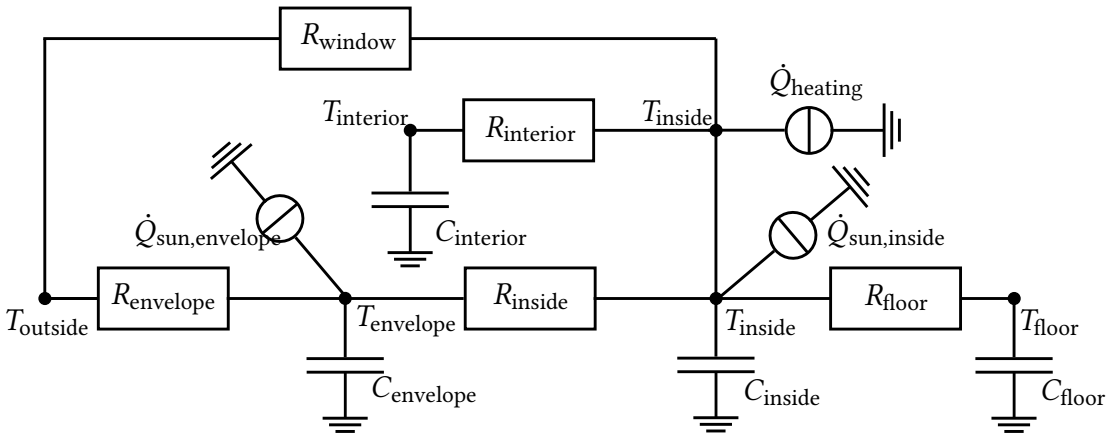

Figure 3.2. Structure of the thermal model in RC- analogy

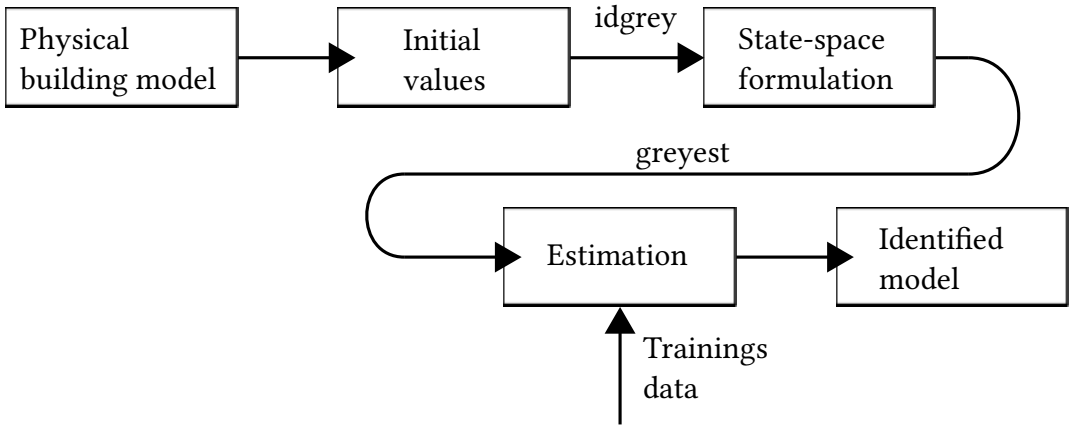

Figure 3.3. Work flow of grey-box modelling with Matlab

Summarising, Figure 3.2 illustrates the building model with all its connections according to the RC- analogy.

3.3.1. Parameter identification

Figure 3.3 explains the procedure, how to generate the grey-box model from the physical building model.
The used toolbox from Matlab is the "System Identification Toolbox". For this application, the most important commands are "idgrey" and "greyest". With the idgrey-command, we can specify the building model as the initial model for the grey-box estimation in state-space formulation. That means the thermal resistances and capacitance, which we determined above, are the initial values for the estimation and they are the values, which the estimator

from Matlab can vary. We add also the parameters $f_{\text{sol,inside}}$ and $f_{\text{sol,envelope}}$ for estimating because we model in the simplest way the heat flow of the sun isolation $\dot{Q}_{\text{sun,envelope}}$ and $\dot{Q}_{\text{sun,inside}}$ with the measured diffuse insolation I_{sun} (see the following equation).

$$\begin{aligned} \dot{Q}_{\text{sun,inside}} &= f_{\text{sol,inside}} I_{\text{sun}} \\ \dot{Q}_{\text{sun,envelope}} &= f_{\text{sol,envelope}} I_{\text{sun}} \end{aligned} \tag{3.8}$$

The initial values for $f_{\text{sol,inside}}$ and $f_{\text{sol,envelope}}$ are chosen as 0.25 according to Harb et al. [50]. And, we replace in the differential equation of the envelope temperature from Equation 3.4 the thermal resistance R_{inside} to R_{in}. The initial values of R_{inside} and R_{in} are the same, but we obtain more flexibility in the grey-box model, if we estimate both values.
After that, we look for the data from the reference building. The data are generated in an experiment, but this is explained in a subsequent chapter. When we have the data, they are separated into training data and verification data. The training data are used for the estimation. From the reference building, we obtain the room temperatures, which we average with the capacitance of each room to one value, the inside temperature. The same procedure is adopted for the outer wall temperature, except that the outer wall temperatures are averaged with their own capacitance. The interior and the floor temperatures are determined in the same way. Also, we obtain data of the heating system for $\dot{Q}_{\text{heating}}$ and the weather specially the outside temperature T_{outside} and the diffuse insolation I_{sun} for determining $\dot{Q}_{\text{sun,envelope}}$ or $\dot{Q}_{\text{sun,inside}}$.
Now, the greyest-command executes the parameter identification with the training data. The used search method of the greyest-command is subspace Gauss-Newton least squares search. The table below summarizes the modelling parameters for the estimation. The states T_{inside} and T_{envelope} are also defined as the output to be optimized. For the later MPC, T_{inside} is the only relevant output. However, we expect better results for the whole model during optimizing the two states with the more complex differential equations. At last, we obtain the ready model (see in section A.1 the initial values and the identified values).

3.3.2. Training and verification of the thermal model

The training data set comprise twelve days from 23 July to 4 August 2021, including a heating period from 26 July to 1 August 2021. The verification data set is half the size of the training data set (from 13 July to 19 July 2021), also including a heating period from 16 July to 18 July

Parameters to be identified	C_{inside}, C_{envelope}, C_{interior}, C_{floor}, R_{inside}, R_{window}, R_{envelope}, R_{interior}, R_{floor}, R_{in}, $f_{\text{sol,inside}}$, $f_{\text{sol,envelope}}$
Inputs	$\dot{Q}_{\text{heating}}$, I_{sun}, T_{outside}
Outputs to be optimized	T_{inside}, T_{envelope}

Table 3.5. Conclusion of relevant information about the grey-box model

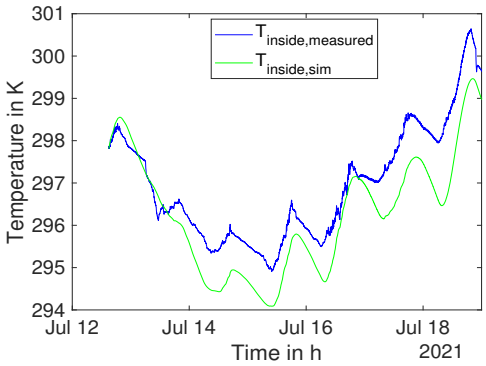

Figure 3.4. Verification of the building model

2021.

Figure 3.4 shows the curve of the inside temperature of the simulated and the measured values. It is noticeable that the model reflects the dynamic of reality sufficiently. In addition, the Root Mean Square Error (RMSE) and the maximum residual (R_{max}) is used as verification measure of the model.

The RMSE is calculated with the quadratic difference of the simulated output y_{sim} and the measured output y_{meas} as follows [51]:

$$RMSE = \sqrt{\frac{1}{N}\sum_{1}^{N}(y_{\text{sim}} - y_{\text{meas}})^2} \tag{3.9}$$

Here is N the number of measurements or simulated values. Based on the Figure 3.5 presented RSME and R_{max}, it can be shown that during the training and verification period, the magnitudes of the RSME and R_{max} are similar. The results of the RMSE and the R_{max} are listed for the two optimized outputs after the training and the verification period. The maximum difference between the training and verification period for the RMSE lies by 0.3 K and for the R_{max} by 0.19 K. As a result, we can verify the building model.

	T_{inside}		T_{envelope}	
RMSE	0.61 K	0.59 K	0.49 K	0.52 K
R_{max}	1.45 K	1.62 K	1.22 K	1.03 K

Training period
Verification period

Figure 3.5. RMSE and R_{max} of the output for training and verification period

3.4. The state-space formulation

The white-box model of the water reservoir and the grey-box model of the building behaviour have now been prepared. In the next step, we put them together in the state-space formulation, which we introduced in subsection 2.3.2, just as the MPC requires.
The separation in control signal **u** and disturbances **d** is important for this. The control signals are the heat flow of the heating system and the heat pump in the reference building. The main disturbances are the weather and, especially for the water reservoir, heat losses. Therefore, the state-space formulation looks as follows:

$$\begin{pmatrix} \frac{dT_{inside}}{dt} \\ \frac{dT_{envelope}}{dt} \\ \frac{dT_{interior}}{dt} \\ \frac{dT_{floor}}{dt} \\ \frac{dU_{WR}}{dt} \end{pmatrix} = A \begin{pmatrix} T_{inside} \\ T_{envelope} \\ T_{interior} \\ T_{floor} \\ U_{WR} \end{pmatrix} + B_1 \begin{pmatrix} \dot{Q}_{heating} \\ \dot{Q}_{HP} \end{pmatrix} + B_2 \begin{pmatrix} I_{sun,inside} \\ I_{sun,envelope} \\ T_{outside} \\ \dot{Q}_{loss} \end{pmatrix} \tag{3.10}$$

$$T_{inside} = C \begin{pmatrix} T_{inside} \\ T_{envelope} \\ T_{interior} \\ T_{floor} \\ U_{WR} \end{pmatrix}$$

The hole matrices A, B_1, B_2, and C are in section A.2. We have no pass-through matrices because neither control signals nor disturbances have a direct impact on the output.

4. Experiments

In the section 3.3 is described how the grey-box model of the building is created. However, it is not nearly explained where the data comes from. Experiments have been conducted specifically to obtain this data. These experiments are explained in this separate chapter.
This thesis is developed during the summer, thus no data from the reference building with a non-zero control signal $\dot{Q}_{\text{heating}}$ are available. To acquire data with the varying control signal, we heat the reference building with electric heaters in two experiments, one for verification data and one for training data. Therefore, the sensors of the building record the temperature curves in the rooms and the electrical consumption of the building. The experiments are under the assumption that the whole electrical power of the heaters and other consumers of power, such as lights and office devices, is changed in heat.

4.1. Experiment 1

The feasibility of the first experiment on the reference building is unclear. To be able to simply repeat the experiment in the event of an error, the experiment with the smaller data set is conducted at first. Hence, the first experiment aims to obtain the data for the verification period, which is shorter than the training period. Furthermore, the experiment is conducted over a weekend (from 16. July to 18. July 2021), as we reduce interference from occupants, such as opening doors or windows, and we enable the occupants a comfortable working temperature. Therefore, all windows and doors are opened after the experiment to cool down the building. At last, there should be no electrical charging of the cars during the experiment, because this electricity consumption has the same measuring point as the electricity consumption of the entire building. This would disrupt the assumption that all electrical power is converted into heat.
At first, we set up the household heater without a fan in room 1, the household heater with a fan in room 2, and the industrial heater in floor 2 (see Figure 2.4). The heaters are

Heater	Acronym	Technical data	Configuration
Household Heater without a Fan	HoHe	• maximum power: 2000W • closed-loop control	• switch symbol: | • temperature setting: $5-6$
Household Heater with a Fan	HoHeF	• maximum power: 2000W • open-loop control	• switch symbol: 750W
Industrial Heater	IH	• maximum power: 9000W • closed-loop control	• switch symbol: ▬ • temperature setting: middle

Table 4.1. Technical data and configuration during the experiments

selected based on availability so that no new equipment has to be purchased. Some technical information and the configuration of the heaters are described in Table 4.1.

4.1.1. Data of the experiment 1

A more exact sequence of the experiment is showing in Table A.2 as laboratory journal or in the Figure 4.2 with the data. The Figure presents the electrical consumption P_el and the air temperatures in rooms 1 and 2, the kitchen, and floor 2 of the reference building from the beginning to the ending of the experiment. The start is marked by switching on the heaters in floor 2 and rooms 1 and 2. In the end, the heaters are switched off in room 1, the kitchen and floor 2.
The data demonstrate the behaviour of the heaters. Consequently, in floor 2, the IH switches often on and off due to the closed-loop control. Therefore, IH generates the fluctuations in the increasing air temperature curve. At the same time, we notice the on and off of the heater in P_el at the high peaks. The HoHe has the same behaviour as the IH but with a smaller influence on the air temperature in room 1 due to its lower power.
Only the HoHeF is controlled open-loop and heats constantly with 750W the room air, where we remark no fluctuations in the temperature rise. Because the HoHeF does not switch off

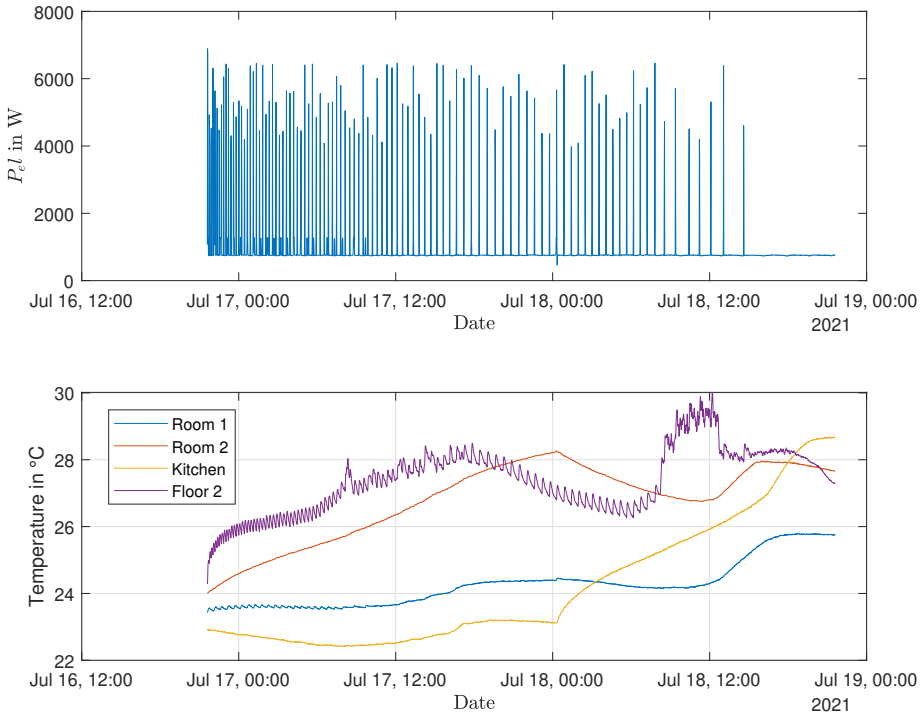

Figure 4.1. Electrical consumption of the building and air temperature inside the rooms during the experiment 1

independently and we have sunny days during the experiment, some temperatures, e.g. the screed temperature, are nearly below 40°C. To avoid a too-hot room for the occupants after the experiment, we stop heating room 2 on Saturday night and rearrange the HoHeF in the kitchen. Since we average the temperature in all rooms for the model estimation from chapter 3, it is not relevant which room is heated.

4.2. Experiment 2

The experiment 2 roots also on the general assumption of changing the entire electrical power to heat. In contrast to experiment 1, we have several heating periods as we heat on working days during the night and on the weekend in order to generate a longer training data set. In order not to burden the occupants during the working day, we heat at night and heat the kitchen that is not in use.

Programmable logic controller (PLC)

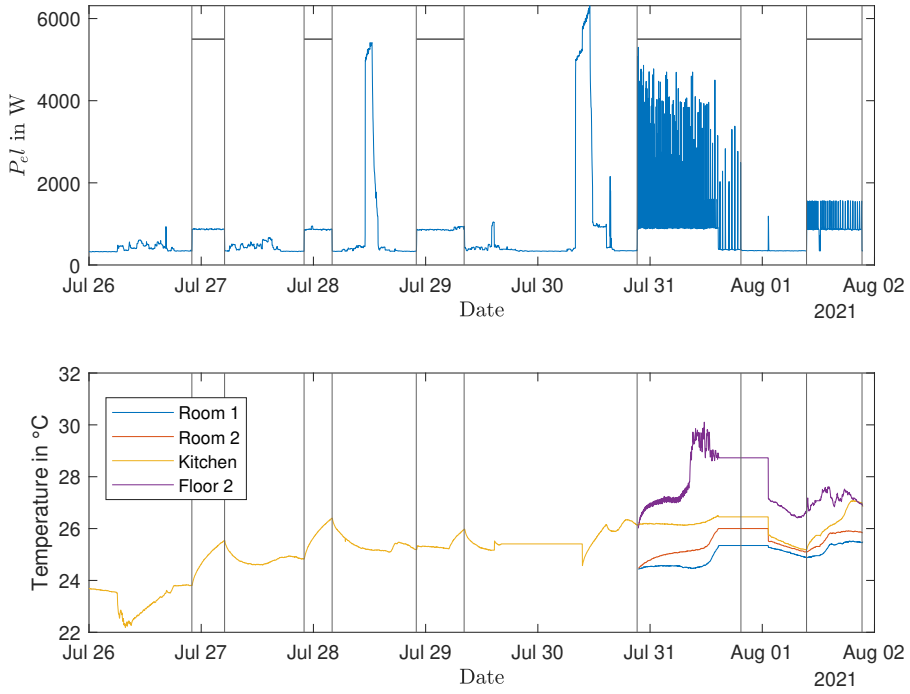

Figure 4.2. Electrical consumption of the building and air temperature inside the rooms during the experiment 1

4.2.1. Data of the experiment 2

4.3. Findings of the experiments

5. Model predictive control

5.1. Optimization

5.2. Constrains

5.3. Cost function

6. Results

7. Conclusion

8. Outlook

Bibliography

[1] United Nations. *Paris Agreement*. 2015.

[2] Deutschlandfunk, ed. *Auf dem Weg zur Klimaneutralität: Die neuen Klimaziele für Deutschland*. 24.06.2021.

[3] Bundesregierung. *Abschied von der Kohleverstromung: Fragen und Antworten*. Ed. by Presse- und Informationsamt der Bundesregierung. 2021.

[4] C. W. Gellings. *The concept of demand-side management for electric utilities*. In: *Proceedings of the IEEE*, Vol. 73, No. 10 (1985), pp. 1468–1470.

[5] Karl-Heinz Backhaus (Vaillant), Dr. Hendrik Ehrhardt (Stiebel Eltron), André Jacob (BWP), Barbara. *Branchenstudie 2021: Marktanalyse - Szenarien - Handlungsempfehlungen: Vorabveröffentlichung zum*. In: (24.11.2020).

[6] R. Kramer, J. van Schijndel, and H. Schellen. *Simplified thermal and hygric building models: A literature review*. In: *Frontiers of Architectural Research*, Vol. 1, No. 4 (2012), pp. 318–325.

[7] J. Široký, F. Oldewurtel, J. Cigler, and S. Prívara. *Experimental analysis of model predictive control for an energy efficient building heating system*. In: *Applied Energy*, Vol. 88, No. 9 (2011), pp. 3079–3087.

[8] I. Hazyuk, C. Ghiaus, and D. Penhouet. *Optimal temperature control of intermittently heated buildings using Model Predictive Control: Part I – Building modeling*. In: *Building and Environment*, Vol. 51 (2012), pp. 379–387.

[9] H. Park, M. Ruellan, A. Bouvet, E. Monmasson, and R. Bennacer. *Thermal parameter identification of simplified building model with electric appliance*. In: *11th International Conference on Electrical Power Quality and Utilisation (EPQU), 2011*. Piscataway, NJ: IEEE, 2011, pp. 1–6.

[10] S. Freund and G. Schmitz. *Entwicklung und Validierung von Grey-Box-Modellen zur Modellierung des thermischen Verhaltens von Einzelbüros in einem Niedrigenergie-Bürogebäude.* In: (2020).

[11] Evelyn Sperber. *Grey-Box-Modellierung des thermischen Verhaltens von Typgebäuden.* 11. Internationale Energiewirtschaftstagung. 2019.

[12] D. Coakley, P. Raftery, and M. Keane. *A review of methods to match building energy simulation models to measured data.* In: *Renewable and Sustainable Energy Reviews*, Vol. 37 (2014), pp. 123–141.

[13] Jiří Cigler, Jaň Sirok, Milan Korda, and Colin N Jones. *On the Selection of the Most Appropriate MPC Problem Formulation for Buildings.* In: (2013).

[14] I. Hazyuk, C. Ghiaus, and D. Penhouet. *Optimal temperature control of intermittently heated buildings using Model Predictive Control: Part II – Control algorithm.* In: *Building and Environment*, Vol. 51 (2012), pp. 388–394.

[15] P. Zwickel, A. Engelmann, L. Groll, V. Hagenmeyer, D. Sauer, and T. Faulwasser. *A Comparison of Economic MPC Formulations for Thermal Building Control.* In: *2019 IEEE PES Innovative Smart Grid Technologies Europe (ISGT-Europe).* IEEE, 29.09.2019 - 02.10.2019, pp. 1–5.

[16] F. Oldewurtel, A. Ulbig, A. Parisio, G. Andersson, and M. Morari. *Reducing peak electricity demand in building climate control using real-time pricing and model predictive control.* In: (2010), pp. 1927–1932.

[17] Danny Günther, Jeannette Wapler, Robert Langner, Sebastian Helmling, Dr.-Ing. Marek Miara, Dr.-Ing. David Fischer, Dirk Zimmermann, Tobias Wolf, Dr.-Ing. Bernhard Wille-Hausmann. *Wärmepumpen in Bestandsgebäuden: Ergebnisse aus dem Forschungsprojekt "WPsmart im Bestand": Abschlussbericht.* Ed. by Fraunhofer Institut für Solare Energiesysteme ISE. Freiburg, 2020.

[18] P. Kohlhepp and V. Hagenmeyer. *Technical Potential of Buildings in Germany as Flexible Power-to-Heat Storage for Smart-Grid Operation.* In: *Energy Technology*, Vol. 5, No. 7 (2017), pp. 1084–1104.

[19] M. Avci, M. Erkoc, A. Rahmani, and S. Asfour. *Model predictive HVAC load control in buildings using real-time electricity pricing.* In: *Energy and Buildings*, Vol. 60 (2013), pp. 199–209.

[20] G. Bianchini, M. Casini, D. Pepe, A. Vicino, and G. G. Zanvettor. *An integrated model predictive control approach for optimal HVAC and energy storage operation in large-scale buildings*. In: *Applied Energy*, Vol. 240, No. 1 (2019), pp. 327–340.

[21] D. Kim and J. E. Braun. *Hierarchical Model Predictive Control Approach for Optimal Demand Response for Small/Medium-sized Commercial Buildings*. In: (2018), pp. 5393–5398.

[22] G. Bianchini, M. Casini, A. Vicino, and D. Zarrilli. *Demand-response in building heating systems: A Model Predictive Control approach*. In: *Applied Energy*, Vol. 168, No. 3 (2016), pp. 159–170.

[23] W. Wang, J. Zhang, B. Michael, and B. Futrell. *Energy Savings of Occupancy-Based Controls in Office Buildings*. In: (2019), pp. 932–939.

[24] X. Liang, T. Hong, and G. Q. Shen. *Occupancy data analytics and prediction: A case study*. In: *Building and Environment*, Vol. 102 (2016), pp. 179–192.

[25] H. D. Baehr and S. Kabelac, eds. *Thermodynamik*. Berlin, Heidelberg: Springer Berlin Heidelberg, 2016.

[26] *VDI-Wärmeatlas*. Berlin, Heidelberg: Springer Berlin Heidelberg, 2013.

[27] H. Kuchling, ed. *Taschenbuch der Physik: Mit zahlreichen Tabellen*. 19., aktualisierte Aufl. München: Fachbuchverl. Leipzig im Carl-Hanser-Verl., 2007.

[28] A. Griesinger, ed. *Wärmemanagement in der Elektronik*. Berlin, Heidelberg: Springer Berlin Heidelberg, 2019.

[29] H. D. Baehr and K. Stephan, eds. *Wärme- und Stoffübertragung*. Berlin, Heidelberg: Springer Berlin Heidelberg, 2016.

[30] L. Grüne and J. Pannek. *Nonlinear model predictive control: Theory and algorithms*. Second edition. Communications and control engineering. Cham: Springer, 2017.

[31] J. T. Wen and S. Mishra, eds. *Intelligent Building Control Systems: A Survey of Modern Building Control and Sensing Strategies*. Advances in Industrial Control. Cham: Springer, 2018.

[32] F. Oldewurtel, A. Parisio, C. N. Jones, D. Gyalistras, M. Gwerder, V. Stauch, B. Lehmann, and M. Morari. *Use of model predictive control and weather forecasts for energy efficient building climate control*. In: *Energy and Buildings*, Vol. 45, No. 9 (2012), pp. 15–27.

[33] B. Kouvaritakis and M. Cannon, eds. *Model Predictive Control*. Cham: Springer International Publishing, 2016.

[34] Karlsruher Institut für Technologie. *Energy Lab 2.0*. https://www.elab2.kit.edu/index.php, 15.07.2021.

[35] Bundesverband Wärmepumpe e.V. *Positives Signal für den Klimaschutz: 40 Prozent Wachstum bei Wärmepumpen*. 19.01.2021.

[36] ratiotherm Smart Energy Systems, ed. *Technische Daten: Oskar°Wärmepumenspeicher WPS*.

[37] Udo Machauer. *Bauplan_Wärmepumpenhaus*. Ed. by Karlsruher Institut für Technologie. 2017.

[38] Statusseminar. Forschung für Energieoptimiertes Bauen, ed. *Modellbasierte Betriebsanalyse von Gebäuden - Methoden für die Fehlererkennung und Optimierung im Gebäudebetrieb*. 2009.

[39] S. Estrada-Flores, I. Merts, B. DE Ketelaere, and J. Lammertyn. *Development and validation of "grey-box" models for refrigeration applications: A review of key concepts*. In: *International Journal of Refrigeration*, Vol. 29, No. 6 (2006), pp. 931–946.

[40] Andreas Kejzlar. *Roth Flächentemperierung: Roth_Auslegung_Fbh*. Ed. by Roth Energiesysteme Sanitärsysteme. 21.01.2020.

[41] SEF Ingenieurgesellschaft MBH. *KÜHLLASTBERECHNUNG VDI 2078*. 5.09.2019.

[42] IDM ENERGIESYSTEME GMBH. *Technische Unterlagen Montageanleitung: AERO SLM 3- 11 AERO SLM 6- 17: Zusätzliche Ausstattungsvarianten HGL ohne HGL*.

[43] B. Weigand, J. Köhler, and J. VON Wolfersdorf, eds. *Thermodynamik kompakt – Formeln und Aufgaben*. Berlin, Heidelberg: Springer Berlin Heidelberg, 2016.

[44] Anton Schweizer. *Formelsammlung und Berechnungsprogramme Maschinen- und Anlagenbau: Wärmeübergangskoeffizienten - Gase - Luft -*. Ed. by Schweizer-fn.

[45] Thorben Frahm. *Ein Fenster mit niedrigem U-Wert spart Energie*. Ed. by D. UND Sanieren. 2021.

[46] Anton Schweizer. *Formelsammlung und Berechnungsprogramme Maschinen- und Anlagenbau: Wärmeleitfähigkeit verschiedener Matereialien*. Ed. by Schweizer-fn. 12.10.2021.

[47] K. Ghazi Wakili, E. Hugi, L. Karvonen, P. Schnewlin, and F. Winnefeld. *Thermal behaviour of autoclaved aerated concrete exposed to fire.* In: *Cement and Concrete Composites*, Vol. 62, No. 283 (2015), pp. 52–58.

[48] Abteilung Klima- und Umweltberatung. *Jahresmittel der Windgeschwindigkeit - 10 m über Grund - in Baden-Württemberg: Statistisches Windfeldmodell (SWM).* Offenbach, 2004.

[49] Anton Schweizer. *Formelsammlung und Berechnungsprogramme Maschinen- und Anlagenbau: Wärmekapazität verschiedener Materialien.* Ed. by Schweizer-fn. 12.10.2021.

[50] H. Harb, N. Boyanov, L. Hernandez, R. Streblow, and D. Müller. *Development and validation of grey-box models for forecasting the thermal response of occupied buildings.* In: *Energy and Buildings*, Vol. 117, No. 6 (2016), pp. 199–207.

[51] A. G. Barnston. *Correspondence among the Correlation, RMSE, and Heidke Forecast Verification Measures; Refinement of the Heidke Score.* In: *Weather and Forecasting*, Vol. 7, No. 4 (1992), pp. 699–709.

Nomenclature

Acronyms

DSM Demand Side Management

HoHe Household Heater without a fan

HoHeF Household Heater with a Fan

HP Heat Pump

HVAC Heating, Ventilation, and Air Conditioning

IH Indusrial Heater

KIT Karlsruhe Institute of Technology

MPC Model Predictive Control

RMSE Root Mean Square Error

SW Service Water

UN United Nations

WR Water Reservoir

Greek letters

α	heat transfer coefficient	$W/(m^2K)$
λ	thermal conductivity	$W/(mK)$

Physical size

ΔT	temperature difference	K

$\partial T/\partial x$	temperature gradient	K/m
U	inner energy	J

	Initial values	Identified values
C_{inside}	400425 J/W	1198069 J/W
C_{envelope}	24999045 J/W	24998057 J/W
C_{interior}	22960754 J/W	22960750 J/W
C_{floor}	26118734 J/W	26118731 J/W
R_{inside}	191 K/W	0,66 K/W
R_{window}	34 K/W	0.0025 K/W
R_{envelope}	287 K/W	0,00008 K/W
R_{interior}	77 K/W	28001 K/W
R_{floor}	749 K/W	2719 K/W
R_{in}	191 K/W	191 K/W
$f_{\text{sol,inside}}$	0,25	7.80685 K/W
$f_{\text{sol,envelope}}$	0,25	-7.30632 K/W

Table A.1. Initial and identified values of the model parameters

A. Appendix

A.1. Model values

A.2. Matrices of state-space formulation

$$B_1 = \begin{pmatrix} 1 & 0 \\ 0 & 0 \\ 0 & 0 \\ 0 & 0 \\ -1 & 1 \end{pmatrix} \tag{A.1}$$

A. Appendix

$$B_2 \begin{pmatrix} f_{sun,inside} & 0 & \frac{1}{C_{inside}R_{window}} & 0 \\ 0 & f_{sun,envelope} & \frac{1}{C_{envelope}R_{envelope}} & 0 \\ 0 & 0 & 0 & 0 \\ 0 & 0 & 0 & 0 \\ 0 & 0 & 0 & -1 \end{pmatrix} \tag{A.2}$$

$$C = \begin{pmatrix} 1 & 0 & 0 & 0 & 0 \end{pmatrix} \tag{A.3}$$

$$
A = \begin{pmatrix}
\frac{-1}{C_{inside}R_{inside}} - \frac{1}{C_{inside}R_{window}} - \frac{1}{C_{inside}R_{interior}} - \frac{1}{C_{inside}R_{floor}} & \frac{1}{C_{inside}R_{inside}} & \frac{1}{C_{inside}R_{interior}} & \frac{1}{C_{inside}R_{floor}} \\
\frac{1}{C_{envelope}R_{inside}} & \frac{-1}{C_{envelope}R_{envelope}} - \frac{1}{C_{envelope}R_{inside}} & 0 & 0 \\
\frac{1}{C_{interior}R_{interior}} & 0 & -\frac{1}{C_{interior}R_{interior}} & 0 \\
\frac{1}{C_{floor}R_{floor}} & 0 & 0 & -\frac{1}{C_{floor}R_{floor}} \\
0 & 0 & 0 & 0
\end{pmatrix} \tag{A.4}
$$

A.3. Laboratory journal

Experiment: 16. July - 18. July 2021

Time	Location	Incident
16.7.21 9.30pm	Room 1	HoHe on
	Room 2	HoHeF on
	FOG	IH on
		closed doors
18.7.21 0.00am	Room 2	HoHeF off
		rearrange HoHeF
	Kitchen	HoHeF on
18.7.21 9.30pm	Room 1	HoHe off
	Kitchen	HoHeF off
	FOG	IH off
		opened doors and windows

Table A.2. Laboratory journal: 16. July - 18. July 2021

Experiment: 16. July - 18. July 2021

Time	Location	Incident
26.7. - 27.7.21	Kitchen	HoHeF on
10.00pm - 5.00am		closed door
27.7. - 28.7.21	Kitchen	HoHeF on
10.00pm - 4.00am		closed door
28.7. - 29.7.21	Kitchen	HoHeF on
10.00pm - 5.00am		opened door
5.00am - 8.20am		closed door
29.7. - 30.7.21	all	breakdown PLC
16.00pm - 9.30am	Kitchen	HoHeF still off
30.7.21 9.30pm	Room 1	HoHe on
	Room 2	HoHeF on
	FOG	IH on
		opened doors
31.7. - 1.8.21	all	breakdown PLC
2.30pm - 9.20am		
31.7.21 4.00pm	Room 1	HoHe off
	Room 2	HoHeF off
7.30pm	FOG	IH off
1.8.21 9.30pm	Room 1	HoHe on
	Kitchen	HoHeF on
		PLC works
1.8.21	all	breakdown PLC
11.30am - 0.20pm		
1.8.21 9.30pm	Room 1	HoHe off
	Kitchen	HoHeF off
	FOG	IH off
		opened doors and windows

Table A.3. Laboratory journal: 26. July - 1. August 2021

Figure A.1. A figure

A. Appendix

…